

# Modelling M/M/R-JSQ-PS sojourn time distribution for Ultra-Reliable Low Latency Communication services

Geraint I. Palmer<sup>a,\*</sup>, Jorge Martín-Pérez<sup>b</sup>

<sup>a</sup>*School of Mathematics, Cardiff University, Senghennydd Road, Cardiff, CF24 4AG, Wales*

<sup>b</sup>*Department of Telematics Engineering, Universidad Carlos III de Madrid, Av. de la Universidad, Leganés, Spain*

## ARTICLE INFO

**Keywords:**  
queueing  
simulation

## ABSTRACT

The future Internet promises to support time-sensitive services that require ultra low latencies and reliabilities of 99.99%. Recent advances in cellular and WiFi connections enhance the network to meet high reliability and ultra low latencies. However, the aforementioned services require that the server processing time ensures low latencies with high reliability, otherwise the end-to-end performance is not met. To that end, in this paper we use queuing theory to model the sojourn time distribution for Ultra-Reliable Low Latency Communication services of M/M/R-JSQ-PS systems: Markovian queues with  $R$  CPU servers following a join shortest queue processor-sharing discipline (for example Linux systems). We develop open-source simulation software, and develop and compare six analytical approximations for the sojourn time distribution. The proposed approximations yield Wasserstein distances below 2 time units, and upon medium loads incur into errors of less than 1.78 time units (e.g., milliseconds) for the 99.99<sup>th</sup> percentile sojourn time. Moreover, the proposed sojourn time approximations are stable regardless the number of CPUs and stay close to the simulations.

## 1. Introduction

Recent advances in the networking community aim at a better control over infrastructure behaviour. Although the Internet was designed to provide a best-effort delivery (Kempf, IAB and Austein, 2004), 5G (3GPP, 2019a), WiFi 6 (IEEE, 2021b,a) and WiFi 7 (IEEE, 2021a) have enhanced the mobile connectivity to increase the network reliability. With the new wireless technologies it is possible to support services that require low latencies and high reliabilities like vehicle to everything (V2X) (5G Americas, 2021), drones control (Albanese et al., 2021), remote surgery (Acemoglu et al., 2020), or Industry 4.0 (Aschenbrenner et al., 2015). In particular, it is now possible to remotely control an industrial robotic arm over a wireless connection (Guimarães et al., 2021) while guaranteeing a reliable communication.

The 3<sup>rd</sup> Generation Partnership Project (3GPP) claims (3GPP, 2022c) that the aforementioned services require an Ultra-Reliable Low Latency Communication (URLLC) over the Internet. That is, any URLLC service should foresee Internet latencies in the order of 10 ms and reliabilities above a 99%. 5G and WiFi already guarantee a low latency and reliable wireless communication through diverse mechanisms (3GPP, 2021, 2019a,b, 2022b,a), but it is out of their scope whether the processing time of Internet traffic satisfies an URLLC.


Internet packets exchanged by URLLC services are typically processed in a remote server accessible through a 5G or WiFi connection. In a remotely controlled industrial robot (Guimarães et al., 2021) the steps are as follows: (i) the robot reports its position within packets sent over 5G/WiFi to a server; (ii) the server calculates the next robot position; and

(iii) the robot receives an instruction with its new position over the 5G/WiFi connection. Calculating the next robot position at step (ii) induces a processing latency that depends on factors such as the server load, the arrival distribution of sensor data, how fast the server is, how many CPUs the server has, or how complex operations are.

In the case of a remotely controlled robotic arm, the server CPUs perform inverse/forward kinematics (Liu and Khong, 2015) and PID control (Chitta, Sucan and Cousins, 2012) operations to derive the next position of the robotic arm. Both operations are performed at a CPU for each URLLC packet, and their delay is impacted by the number of packets being processed at the same CPU. Hence, if a CPU is attending multiple URLLC packets it is more unlikely that the processing time remains below the latency requirement of 10 ms. Consequently, the latency of a remotely controlled robotic arm may exceed the 10 ms requirement even if the 5G or WiFi 6/7 connection provides URLLC – steps (i) and (iii) in the prior paragraph.

Assuming that a 5G or WiFi 6/7 connection suffices to provide URLLC for a service is not enough. It is also necessary to understand how the processing time is distributed when URLLC traffic is attended by a server. Only when both the URLLC traffic processing and wireless communication satisfy the latency requirements, we can tell that the network infrastructure provides an URLLC service, e.g., that it ensures latencies below 10 ms 99% of probability. Therefore, it is of paramount importance to model the URLLC processing latency.

In this paper we study how the traffic processing latency is distributed to determine whether a service meets URLLC. Specifically, we develop open-source simulation software, and also propose analytical approximations to characterise the processing latency of servers that dispatch the traffic pro-

 palmergi1@cardiff.ac.uk (G.I. Palmer); jmartinp@it.uc3m.es (J. Martín-Pérez)

ORCID(s): 0000-0001-7865-6964 (G.I. Palmer); 0000-0001-9295-1601 (J. Martín-Pérez)

cessing to the least loaded CPU within a pool of  $R$  CPUs. As assumed by the state of the art (Cohen, Lewin-Eytan, Naor and Raz, 2015; Jemaa, Pujolle and Pariente, 2016; Oljira, Grinnemo, Taheri and Brunstrom, 2017); and alike Linux-based systems, we assume that each CPU utilises a processor-sharing policy to attend the traffic processing.

The contributions of our work are summarised as follows:

- We build a discrete event simulation for G/G/R-JSQ-PS systems;
- We propose six analytical approximations for the sojourn time cumulative distribution function (CDF) of M/M/R-JSQ-PS systems;
- We derive a run-time complexity analysis to obtain the sojourn time CDF using both the simulation and analytical approximations;
- We study which approximation is more accurate depending on the system load and number of CPUs;
- We study the accuracy of the best approximation for the latency percentiles required by URLLC services, i.e., from the 99<sup>th</sup> percentile to the 99.999<sup>th</sup> percentile.

In terms of Wasserstein distance, the proposed analytical approximations deviate less than a 2 out of 182 time units from the sojourn time CDF in M/M/R-JSQ-PS systems. For the 99.99<sup>th</sup> percentile, the best approximation yields an error of less than 1.78 time units.

The paper is structure as follows. In Section 2 we introduce the considered system that we study in this paper. Then, in Section 3 we go over the related work about the sojourn time CDF in queueing systems. Later, in Section 4 we discuss the development of the G/G/R-JSQ-PS simulation, and in Section 5 we detail the analytical approximations that we propose for the sojourn time CDF of M/M/R-JSQ-PS systems. Afterwards, in Section 6 and Section 7 we study the run-time complexity and accuracy of the proposed approximations, respectively. Then, in Section 8 we study the accuracy of our approximations at the percentiles required by URLLC services. Finally, in Section 9 we conclude our work and point out future research directions.

## 2. An M/M/R-JSQ-PS queueing system

This work is concerned with the sojourn time distribution  $\mathbb{P}(T \leq t)$  of customers in an M/M/R-JSQ-PS system, that is a system with  $R$  parallel processor-sharing queues, with overall Poisson arrival rate  $\Lambda$ , and intended service times distributed exponentially with rate  $\mu$ . Customers join the processor-sharing queue that has the least amount of customers.

Processor-sharing (PS) is a queueing discipline where all customers are served simultaneously, but the service load is shared between the customers. That is, if a customer is expecting to receive a service time  $s$ , then the rate at which that service is given is  $s/n$  when there are  $n$  customers present.

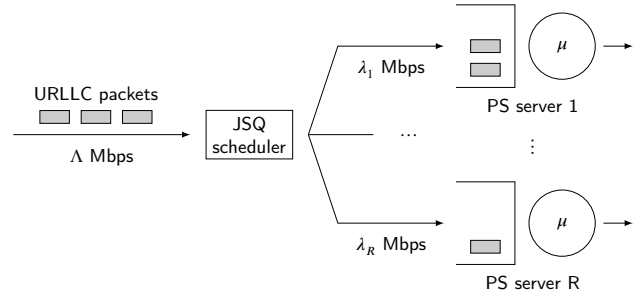


Figure 1: M/M/R-JSQ-PS system processing URLLC packets.

Therefore if there are  $n$  customers present throughout the customer's service, then it will last  $sn$  time units. A key feature is that  $n$  can vary during that customer's service.

Figure 1 illustrates this system. Note that URLLC packets can be considered as customers in the context of queueing theory, hence, throughout the paper we refer to customers as it a standard term in queueing theory.

## 3. Related work

In the networking community queueing theory is a well-established tool to assess the modelling of network infrastructure (Kleinrock, 1977; Harchol-Balter, 2013). The packet-based nature of the Internet, so as the buffering and processor-sharing nature of servers, make it a useful theoretical tool to derive insights on the behaviour of the network. Recent URLLC services and their urgent need for communication guarantees can benefit from the theoretical results of queueing theory in order to adequately evaluate the network performance.

The fundamental results of queueing theory (Kleinrock, 1977) give closed-form formulas for the sojourn time (waiting plus service time) of M/M/1 systems, i.e. systems with 1 server that has exponential service time to dispatch customers arriving according to a Poisson distribution and queue up before they are served. Namely, it is possible to find both the average and CDF for the sojourn time of M/M/1 systems, with the latter having also an exponential distribution (Kleinrock, 1977).

However, the internet traffic is typically dispatched in parallel by multiple servers or CPUs within a server. Hence, it is better resorting to M/M/R systems with up to  $R$  servers (or CPUs) that attend customers in parallel. For such systems, the queueing theory fundamentals also give closed-form expressions for the average sojourn time (Kleinrock, 1977), and indications on how to derive its CDF (Harchol-Balter, 2013).

But still, both M/M/1 and M/M/R systems may not be suitable to model networking components. Either because the assumption of Poissonian arrivals is not suitable or because considering exponential service times is not realistic. To that end, the literature has devoted effort to derive the sojourn time CDF expressions of systems not satisfying such assumptions. For example (Egorova, Zwart and

Boxma, 2006; Ott, 1984) provide expressions for the sojourn time CDFs of M/D/1 and M/G/1 systems, respectively. However both works provide the sojourn time CDF expression in the form of the Laplace-Stieltjes transform, i.e. a non-closed expression of the sojourn time CDF. Other works such as (Masuyama and Takine, 2003) shift the interest to systems that follow Markovian arrival processes (MAP), rather than Poissonian and provide closed-formulas for the sojourn time CDF in MAP/M/1 systems.

In general, making the assumption of Poissonian arrivals is fair as long as there is a considerable amount of independent flows, as the Palm–Khintchine theorem states (Palm, 1943). Hence, it is reasonable to model data centres as M/G/R systems, as suggested by (Harchol-Balter, 2013). Namely, (Harchol-Balter, 2013) motivates the study of M/M/R systems as server farms for traffic processing, and the book leaves as exercise how to derive the sojourn time CDF of an M/M/R system following the strategy used for M/M/1 systems. Nevertheless, M/M/R systems do not mimic the behaviour of Linux based systems where each CPU shares the computing time using a processor-sharing discipline, rather than the one-at-a-time processing of M/M/R, where packets wait in the queue until a server finishes processing a job. As such, (Gupta, Harchol Balter, Sigman and Whitt, 2007) propose to model web server farms using M/M/R-JSQ-PS systems with jobs joining the CPU with the shortest queue (JSQ), and each CPU serving all its jobs simultaneously via a processor-sharing discipline (here joining the ‘shortest queue’ implies joining the CPU with the smallest current load). The research resorts to single queue analysis (SQA) to provide insights on how the traffic intensity changes depending on the queue occupation at each CPU, so as the average number of jobs at each CPU.

The queuing theory literature has widely studied the sojourn time in different systems, and has managed to find out not only their average sojourn time but also the CDF. However, the latter has only been possible in some systems that do not capture the multiple CPUs with PS fashion of Linux based servers. To the best of our knowledge, the existing literature does not provide expressions to compute the sojourn time CDF in PS multi-processor systems that are close to those servers that will process URLLC traffic. Therefore this paper contributes to the related work by proposing six approximations for the sojourn time CDF of M/M/R-JSQ-PS systems. The proposed approximations are useful to check whether the URLLC traffic processing will meet the 99% or similar guarantees of URLLC with almost negligible latencies in the order of 1-10 milliseconds.

To check the accuracy of the proposed approximations we resort to stochastic simulations of the M/M/R-JSQ-PS system. Discrete-event simulation is a standard technique for the task (Robinson, 2014), with a number of commercial (e.g. Simul8 (SIMUL8 Corporation., 2022) and AnyLogic (The AnyLogic Company, 2022)) and open-source (e.g. Simmer (Ucar, Smeets and Azcorra, 2019), SimPy (Team SimPy, 2022), and Ciw (Palmer, Knight, Harper and Hawa, 2019))

software options. However, to the authors’ knowledge, prior to the work of this paper the listed options do not offer straightforward out-of-the-box ways to simulate processor-sharing servers, requiring bespoke code or modifications. Therefore, another major contribution of this paper is the extension of the Ciw software to be able to simulate various kinds of processor-sharing queues. This work is described in Section 4.

#### 4. Simulation of G/G/R-JSQ-PS

In discrete event simulation a virtual representation of a queueing system is created, and ‘run’ by sampling a number of basic random variables such as arrival dates of customers and intended service times, which interact with one another and the system to emulate the behaviour of the queueing system under consideration. Given a long enough runtime and/or a large enough number of trials, observed statistics will converge to exact values due to the law of large numbers. However due to their stochastic nature convergence may be slow, and depending on the complexity of the system, can be computationally expensive. Here the Ciw library (Palmer et al., 2019) is used, an open-source Python library for conducting discrete event simulation. A key contribution of this work is the adaption of the library to include processor-sharing capabilities, which were included in release v2.2.0: these capabilities include standard processor-sharing, limited processor-sharing as described in (Zhang, Dai and Zwart, 2009), and capacitated processor-sharing as described in (Li, 2011), and their combinations.

Ciw uses the event-scheduling approach to discrete event simulation (Palmer et al., 2019). Here time jumps from event to event in a discrete manner, while events themselves can cause any number of other events to be scheduled, either immediately or at some point in the future. If they are scheduled for the future, then they are called **B**-events, for example the event of a customer beginning service will cause a future scheduled event of that customer finishing service. If the events are scheduled immediately, then they are called conditional or **C**-events, for example the event a customer joining a queue may immediately cause another event, that customer beginning service, if there was enough service capacity. In addition to scheduling events, events can cause future events to be re-scheduled for a later or earlier time. A **B**-event, and its scheduling and re-scheduling of future events, is called the **B**-phase; a **C**-event, and its scheduling and re-scheduling of future events is called the **C**-phase; and advancing the clock to the next **B**-event is called the **A**-phase. Figure 2 illustrates this event scheduling process.

Processor sharing is implemented by manipulating the re-scheduling of future events in the following way. Upon arrival, a customer is given an arrival date  $t_*$ , and an intended service time  $s$ . They also observe the number of customers, including themselves, who are present at the processor-sharing server,  $x_*$ . At this point they have already received  $d = 0$  of their intended service time. Given that nothing else changes,

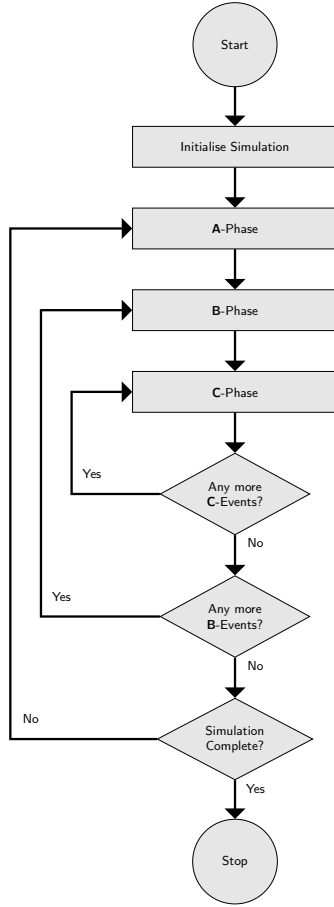


**Figure 2:** Flow diagram of the event scheduling approach used by Ciw, taken from (Palmer, 2018).

this customer will finish service at date  $t_{\text{end}}$  calculated in (1).

$$t_{\text{end}} = t_{\star} + \frac{1}{x_{\star}}(s - d) \quad (1)$$

Therefore this is the date that will be scheduled for that customer to finish service. Now, say an event happens at some  $t$  such that  $t_{\star} < t < t_{\text{end}}$ , and that event is either an arrival to the server, or another customer finishing service with the server. If the event is an arrival, set  $x = x_{\star} + 1$ ; and if the event is a customer finishing service then set  $x = x_{\star} - 1$ . At this point our original customer will have received  $d = d + \frac{1}{x_{\star}}(t - t_{\star})$  of their intended service. Now set  $x_{\star} = x$ ,  $t_{\star} = t$ , and re-calculate their service end date using (1), and then re-schedule their finish service event.

This re-scheduling process is to be performed for every customer in service at any **B**- or **C**- event that causes  $x_{\star}$  to change. This was implemented and released in Ciw v2.2.0, along with some processor-sharing variations: (i) limited processor-sharing queues (Zhang et al., 2009), a generalisation of a processor-sharing queue, in which only a given number of customers may share the service load at any one time; and (ii) capacitated processor-sharing queues (Li, 2011) with a switching parameter, where the service discipline flips

**Table 1**  
Notation table

Symbol	Definition
$T$	random variable for the customer sojourn time
$\Lambda$	overall arrival rate.
$\mu$	intended service rate
$R$	number of parallel processor-sharing servers
$\rho$	traffic intensity $\rho = \frac{\Lambda}{R\mu}$
$\lambda_n$	arrival rate seen by a server with $n$ customers
$W$	complementary sojourn time CDF: $\mathbb{P}(T > t)$
$w_n$	$W$ with $n$ customers, $w_n(t) = \mathbb{P}(T > t   n)$
$A_n$	probability of joining a server with $n$ customers
$\pi_n$	portion arrivals at a server with $n$ customers
$C(\mathbf{v}, b)$	number of occurrences of $b$ in the vector $\mathbf{v}$
$Z(\mathbf{v}, b)$	set of indices in $\mathbf{v}$ where $b$ occurs
$Q$	system transition matrix, with entries $q_{i,j}$
$p_j$	probability of being in state $j$
$D$	defective infinitesimal generator
$L_1$	maximum number of customers at a server
$L_2$	maximum number of customers at the system
$q_{\text{max}}$	maximum runtime of the simulation
$q_{\text{warmup}}$	warmup time used in the simulation
$t_{\text{max}}$	largest value of $T$ calculated
$\Omega(G, H)$	Wasserstein distance between CDFs $G$ and $H$

from FIFO to processor-sharing if the number of customers exceeds this parameter.

The join-shortest-queue processor-sharing system considered in this paper – see Fig. 1 – is implemented by combining this processor-sharing capability with custom routing (JSQ) using inheritance of Ciw’s modules. An example is given in the documentation: [https://ciw.readthedocs.io/en/latest/Guides/behaviour/ps\\_routing.html](https://ciw.readthedocs.io/en/latest/Guides/behaviour/ps_routing.html). Sojourn time CDFs can then be calculated easily as all customer records are saved, namely, the sojourn time of each customer is derived as  $t_{\text{end}} - t_{\star}$ .

## 5. M/M/R-JSQ-PS sojourn time CDF approximations

In order to find the sojourn time distribution of a join-shortest-queue processor-sharing M/M/R-JSQ-PS queue, we follow an approach outlined in (Gupta et al., 2007), called Single Queue Analysis (SQA). Here, rather than consider the whole M/M/R queue, we consider each server as its own M/M/1-PS queue, with state-dependent arrival rates dependent on the join-shortest-queue mechanism. Let  $\Lambda$  denote the overall arrival rate to the M/M/R-JSQ-PS system, then for each PS server in Fig. 1 their effective state-dependent arrival rate is  $\lambda_n$  when there are  $n$  customers already being served by that server. Table 1 summarizes the notation used throughout this paper.

Now, considering a single server as its own queue, we adapt the methodology developed in (Masuyama and Takine, 2003) to the join-shortest-queue situation. In that paper Theorem 1 gives the sojourn time CDF of a single MAP/M/1-PS queue. A small adaptation, now considering an generic



MAP process state-dependent Markovian arrivals  $\lambda_n$ , gives the sojourn time CDF as:

$$\mathbb{P}(T \leq t) = 1 - \mathbb{P}(T > t) = 1 - W(t) = 1 - \sum_{n=0}^{\infty} A_n w_n(t) \quad (2)$$

where  $A_n$  is the probability of an arriving customer joining the queue when there are  $n$  customers already present, and  $w_n(t)$  is the conditional probability that the sojourn time is greater than  $t$  given that there are  $n$  customers already present at arrival.

We study two approximations each for finding the  $\lambda_n$ ,  $A_n$ , and  $w_n$  for each  $n$ . Then combining these in (2) gives us six approximations of the sojourn time CDF for an M/M/R-JSQ-PS queue.

### 5.1. First approximation of $\lambda_n$

Note first that the arrival rate for each single queue being dependent on the number of customers already present in that queue is a valid assumption: the arrival rates to each individual queue when there are  $n$  customers already present depends on the probability of  $n$  being the smallest number of customers present in all  $R$  of the queues. This however is not straightforward to calculate in isolation of the other  $R$  queues, therefore we resort to approximations.

First we note that  $\lambda_n = \pi_n \Lambda$ , where  $\pi_n$  is the proportion of arrivals a server will receive if they have  $n$  customers already present.

We find  $\pi_n$  by constructing a truncated Markov chain of the M/M/R-JSQ-PS system. Define the state space of the non-truncated Markov chain by

$$S = \{(a_1, a_2, \dots, a_R) \mid \forall a_1, a_2, \dots, a_R \in \mathbb{N}_0\} \quad (3)$$

where  $a_z$  denotes the number of customers with server  $z$ . Order the states and let  $s_i$  be the  $i$ th state. Define the transition rate  $q_{i,j}$  from  $s_i$  to  $s_j$ , for all  $i, j$ , by (4):

$$q_{i,j} = \begin{cases} \mu & \text{if } C(\delta, 0) = R - 1 \wedge C(\delta, -1) = 1; \\ \frac{\Lambda}{C(s_i, \min(s_i))} & \text{if } \delta = C(\delta, 0) = R - 1 \wedge C(\delta, 1) = 1 \\ & \wedge Z(\delta, 1) \subseteq Z(s_i, \min(s_i)); \\ 0 & \text{otherwise,} \end{cases} \quad (4)$$

where  $\delta = s_i - s_j$ ;  $C(\mathbf{v}, b) = |\{z \in \mathbf{v} : z = b\}|$  is a function that counts the number of occurrences of  $b$  in a vector  $\mathbf{v}$ ; and  $Z(\mathbf{v}, b) = \{z : \mathbf{v}_z = b\}$  is the set of indices in  $\mathbf{v}$  where  $b$  occurs. Figure 3 is a representation of the Markov chain when  $R = 2$ . When  $R = 1$  this reduces to an M/M/1 (or equivalently M/M/1-PS) system, and it becomes difficult to represent this system when  $R > 2$ .

Steady-state probabilities can be found numerically by truncating the Markov chain, that is choosing an appropriate  $L_1$  such that  $a_z < L_1$  for all servers  $z$ , and solving  $\mathbf{pQ} = \mathbf{0}$  with  $\mathbf{pe} = 1$ , where  $\mathbf{Q}$  is the transition matrix with entries  $q_{i,j}$  and  $\mathbf{e}$  is the vector of ones.

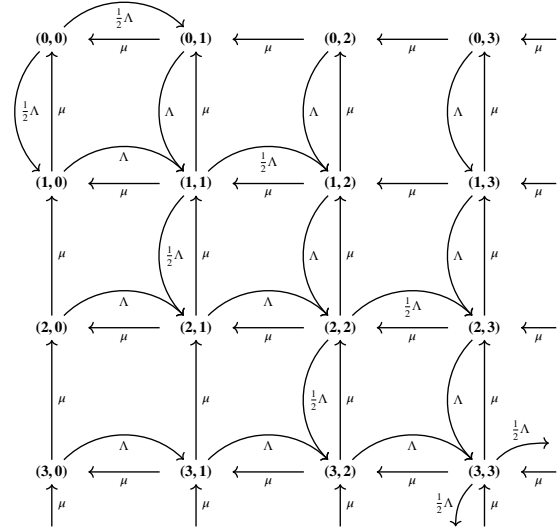


Figure 3: Transition state diagram of the M/M/R-JSQ-PS system when  $R = 2$ .

Once all  $p_i$  are found, the proportion of arrivals a server will receive if it has  $n$  customers already present,  $\pi_n$ , can be found using (5):

$$\pi_n = \left( \sum_{\substack{s_{j,0}=n \\ \min s_j = n}} \frac{p_j}{C(s_j, n)} \right) \left( \sum_{s_{j,0}=n} p_j \right)^{-1} \quad (5)$$

where  $s_{j,0}$  represents the number of customers at the first server when in state  $j$ .

### 5.2. Second approximation of $\lambda_n$

The authors of (Gupta et al., 2007) provide numerical approximations for  $\lambda_0, \lambda_1, \lambda_2$  in (Gupta et al., 2007, Section 5), given in (6), (7) and (8), and all other  $\lambda_n$  for  $n \geq 3$  by (9).

$$\lambda_0 = \mu (k_a - k_b k_c^R - k_d k_e^R) \quad (6)$$

$$\lambda_1 = \frac{\mu \left( \rho^R - 1 + \frac{\mu(\rho - \rho^{R+1})}{\lambda_0(1-\rho)} \right)}{\frac{\lambda_2}{\mu} - \rho^R + 1} \quad (7)$$

$$\lambda_2 = \mu k_f k_g^R \quad (8)$$

$$\lambda_n = \mu \left( \frac{\Lambda}{n\mu} \right)^n \quad (9)$$

with  $k_a, k_b, k_c, k_d, k_e, k_f$  and  $k_g$  defined by:

$$k_a = \frac{\rho}{(1-\rho)} \quad (10)$$

$$k_b = \frac{-0.0263\rho^2 + 0.0054\rho + 0.1155}{\rho^2 - 1.939\rho + 0.9534} \quad (11)$$

$$k_c = -6.2973\rho^4 + 14.3382\rho^3 - 12.3532\rho^2 + 6.2557\rho - 1.005 \quad (12)$$

$$k_d = \frac{-226.1839\rho^2 + 342.3814\rho + 10.2851}{\rho^3 - 146.2751\rho^2 - 481.1256\rho + 599.9166} \quad (13)$$

$$k_e = 0.4462\rho^3 - 1.8317\rho^2 + 2.4376\rho - 0.0512 \quad (14)$$

$$k_f = -0.29\rho^3 + 0.8822\rho^2 - 0.5349\rho + 1.0112 \quad (15)$$

$$k_g = -0.1864\rho^2 + 1.195\rho - 0.016 \quad (16)$$

### 5.3. First approximation of $A_n$

Using the same Markov chain defined in Section 5.1,  $A_n$  can be found by manipulating the steady-state probabilities  $p_n$ , given in (17):

$$A_n = \sum_{\min s_j = n} p_j. \quad (17)$$

### 5.4. Second approximation of $A_n$

From the SQA we can consider each PS server to be its own M/M/1-PS queue with state-dependent arrival rates. This gives a birth-death process, where  $A_n$  is the probability of that system being in state  $n$ . Thus we have:

$$A_n = \prod_{i=0}^{n-1} \frac{\lambda_i}{\mu} A_0 \quad (18)$$

$$A_0 = \left( 1 + \sum_{i=1}^{\infty} \prod_{j=0}^{i-1} \frac{\lambda_j}{\mu} \right)^{-1}. \quad (19)$$

### 5.5. First approximation of $w_n(t)$

Again, we resort to SQA and focus on one server of our M/M/R-JSQ-PS system in Fig. 1. As aforementioned, such server behaves as an M/M/1-PS queue with state-dependant arrivals at rate  $\lambda_n$ , and has a complementary sojourn time CDF  $w_n(t)$  when it is attending  $n$  customers.

We follow the strategy from (Masuyama and Takine, 2003, Section 3), where authors derive  $w_n(t)$  for an MAP/M/1-PS queue. Specifically, we derive  $\mathbf{w}(t) = (w_0(t), w_1(t), w_2(t), \dots)$  as the solution of the differential equation  $\frac{d}{dt}\mathbf{w}(t) = D\mathbf{w}(t)$ , which is:

$$\mathbf{w}(t) = e^{Dt} \mathbf{e} \quad (20)$$

with  $D$  the defective infinitesimal generator for our state-dependant M/M/1-PS queue in the SQA:

$$D = \begin{pmatrix} -(\lambda_0 + \mu) & \lambda_0 & 0 & 0 & \dots \\ \frac{1}{2}\mu & -(\lambda_1 + \mu) & \lambda_1 & 0 & \dots \\ 0 & \frac{2}{3}\mu & -(\lambda_2 + \mu) & \lambda_2 & \dots \\ 0 & 0 & \frac{3}{4}\mu & -(\lambda_3 + \mu) & \dots \\ \vdots & \vdots & \vdots & \vdots & \ddots \end{pmatrix} \quad (21)$$

By constructing a truncated  $D$  explicitly, numerical methods, such as Padé's method (Arioli, Codenotti and Fassino, 1996), are used to find the matrix exponential. As a result,  $w_n(t)$  is obtained as the  $n^{\text{th}}$  entry of the  $\mathbf{w}(t)$  vector in (20).

### 5.6. Second approximation of $w_n(t)$

As constructing  $D$  explicitly and numerically computing a matrix exponential can be computationally inefficient, in Lemma 1 we give a recurrent relation for finding  $w_n(t)$ .

**Lemma 1.** *If a server within an M/M/R-JSQ-PS system has  $n$  customers, its sojourn time CDF is*

$$\mathbb{P}(T > t \mid n) = w_n(t) = \sum_{i=0}^{\infty} \frac{(\lambda_0 + \mu)^i t^i}{i!} e^{-(\lambda_0 + \mu)t} h_{n,i} \quad (22)$$

with  $h_{n,0} = 1$  for all  $n$ ,  $h_{-1,i} = 0$  for all  $i$ , and  $h_{n,i}$  satisfying

$$h_{n,i+1} = \frac{n}{n+1} \frac{\mu}{\lambda_0 + \mu} h_{n-1,i} + h_{n,i} \left( 1 - \frac{\lambda_n + \mu}{\lambda_0 + \mu} \right) + \frac{\lambda_n}{\lambda_0 + \mu} h_{n+1,i} \quad (23)$$

*Proof.* We mimic the proof presented in (Masuyama and Takine, 2003, Corollary 2). and apply the uniformisation technique (Schweitzer, 1996) for the matrix exponential in (20). As a result we obtain:

$$\mathbf{w}(t) = \sum_{i=0}^{\infty} \frac{(\lambda_0 + \mu)^i t^i}{i!} e^{-(\lambda_0 + \mu)t} \left[ I + \frac{1}{\lambda_0 + \mu} D \right]^i \mathbf{e} \quad (24)$$

with  $I$  the identity matrix. To ease the computation of the matrix to the power of  $i$ , (i.e.,  $[\cdot]^i$ ) the following vector is defined  $\mathbf{h}_{n,i} = \left[ I + \frac{1}{\lambda_0 + \mu} D \right]^i \mathbf{e}$ . And it leads to the recursion  $\mathbf{h}_{n,i+1} = \left[ I + \frac{1}{\lambda_0 + \mu} D \right] \mathbf{h}_{n,i}$ , with  $\mathbf{h}_{n,0} = \mathbf{e}, \forall n$ . As a result,  $\mathbf{w}(t)$  is defined as

$$\mathbf{w}(t) = \sum_{i=0}^{\infty} \frac{(\lambda_0 + \mu)^i t^i}{i!} e^{-(\lambda_0 + \mu)t} \mathbf{h}_{n,i} \quad (25)$$

and the  $n^{\text{th}}$  element of  $\mathbf{w}(t)$  is given by (22).  $\square$

This gives  $w_n(t)$  in a form which, for a sufficiently large value,  $L_2$ , in place of infinity, can be found recursively. This naive adaptation of (Masuyama and Takine, 2003) replaces their static MAP with the state-dependent arrival rate  $\lambda_n$ .

### 5.7. Summary & Considerations

In this work we implement and test six different methods of approximating the complementary sojourn time CDF of an M/M/R-JSQ-PS system,  $W(t)$ . Table 2 summarises the methodology.

Choices of model hyper-parameters, those that concern only the methodology and not the system that is itself being modelled, can effect both the accuracy and run-time (or computational complexity) of the model, and choices are usually a compromise between the two. For the Ciw simulation there are three hyper-parameters to consider: the maximum simulation time, the warm up time, and the number of trials. The larger the number of trials, the more we can smooth out the stochastic nature of the DES by take averages of the key performance indicators of each trial, however the

**Table 2**

 Summary of the six methods of calculating  $W(t)$ .

Method	$\lambda_n$	$A_n$	$w_n(t)$
A	5.1	5.3	5.5
B	5.1	5.4	5.5
C	5.2	5.4	5.5
D	5.1	5.3	5.6
E	5.1	5.4	5.6
F	5.2	5.4	5.6

more trials take longer to run. The warm-up time is a proportion of the maximum simulation time where results are not collected. This filtering of results ensures that key performance indicators are not collected before the simulation reaches steady-state, and therefore are not dependent on the starting conditions of the simulation. The larger the warm-up time, the higher the chance that the collected results are in steady state (this is highly dependent on other model parameters), although this means less results to collect and so more uncertainty. A larger maximum simulation time does both, ensures that there are enough results to decrease uncertainty, and increases the chance that steady-state is reached, however this also increases run-times.

Each of the six sub-methods described in Section 5 have hyper-parameters that need to be chosen. Those that explicitly build an infinite Markov chain, that is methods 5.1 and 5.3, need to truncate the Markov chain using a limit  $L_1$ , so that numerical methods can be used on a finite Markov chain. The limit  $L_1$  corresponds to the maximum number of customers each PS server will receive. Thus these Markov chains will have  $L_1^R$  states, and so its construction requires defining  $L_1^{2R}$  transitions. The larger the  $L_1$  the more accurate the model, as there would be a smaller probability of a server receiving more than  $L_1$  customers, however larger limits have longer run-times and larger memory consumption.

Other sub-methods, methods 5.4 and 5.6 contain infinite sums. For these, a sufficiently large cut-off,  $L_2$  is required to truncate these sums for numerical computation. This  $L_2$  corresponds to the overall maximum number of customers that can be present, and so can be chosen to be much larger than  $L_1$ . Similarly, method 5.5 requires the construction of a matrix, where each state corresponds to the overall number of customers, and so  $L_2$  is also used to truncate this matrix.

### 5.8. Markov chain truncation

When we approximate  $\lambda_n$  and  $A_n$  using Section 5.1 and Section 5.3, respectively, we truncate the transition matrix  $Q$  of the Markov chain in (4). Namely, we limit the “last” considered state  $S_i = (L_1 - 1)\mathbf{e}$  has  $L_1 - 1$  users in all the  $R$  servers. The truncation  $L_1$  should be carefully selected such that

$$\sum_{s_j: \max s_j \geq L_1} p_j < \varepsilon \quad (26)$$

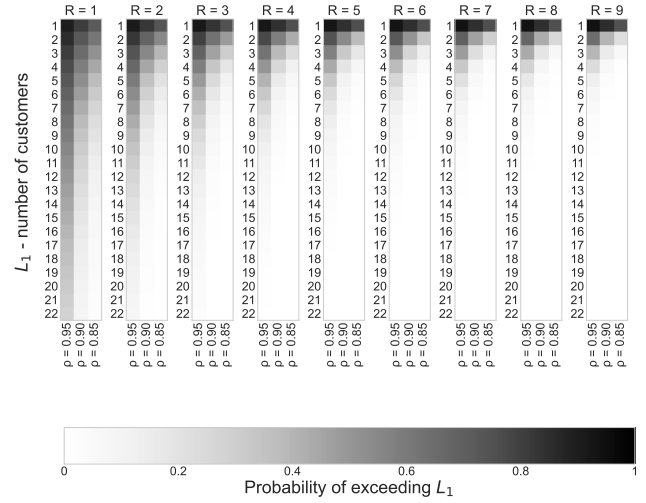


**Figure 4:** Probability of having  $L_1$  or more customers at some server (26) with different loads  $\rho = 0.85, 0.90, 0.95$  and available servers  $R = 1, \dots, 9$ .

that is, the probability of entering a state with a server with  $L_1$  or more customers should remain below a tolerance  $\varepsilon \in \mathbb{R}^+$

Figure 4 illustrates how probability of having  $L_1$  or more users at a server decreases as we increase the truncation limit  $L_1$  and how this is effected by both  $\rho$  and  $R$ . This data was obtained using the simulation described in Section 4.

## 6. Complexity analysis

As stated in the paper title, the main motivation for modelling the M/M/R-JSQ-PS system is to tell whether an URLLC service attended by a multi-processor system meets latency and reliability constraints. Hence, it is of paramount importance to consider the run-time complexity of each approximation  $\lambda_n, A_n, w_n(t)$ , as a network operator may require fast operational decisions to satisfy the URLLC. If the approximation run-time is not fast enough, the operator would not be able to update the operational decisions on time upon demand changes – e.g., increase the dedicated servers to attend the increasing demand for an URLLC service. Therefore, in the following we analyse the run-time complexity of each approximation for  $\lambda_n, A_n$  and  $w_n(t)$ .

### 6.1. First approximation of $\lambda_n$

Using (5) this approximation finds the portion of arrivals that a server foresees using the steady-state probabilities  $p_i$  of the M/M/R-JSQ-R Markov chain with  $L_1^R$  states and transition matrix  $Q$  of size  $L_1^{2R}$ . For each entry  $q_{i,j}$  of the transition matrix we make  $\min(s_i), Z(\delta, b), C(\delta, b)$  operations, all of them of complexity  $\mathcal{O}(R)$ . Hence, computing all entries of the transition matrix  $Q$  takes  $\mathcal{O}(RL_1^{2R})$  operations.

To find the steady-state vector  $\mathbf{p}$  we solve  $(\tilde{Q}\mathbf{e})^T \mathbf{p} = (\mathbf{p}\mathbf{e})^T$ , where  $\tilde{Q}$  is the transition matrix  $Q$  less one row. This is a linear system with a matrix of size  $L_1^R \times L_1^R$ . Finding such solution with the LAPACK (Demmel, 1989) gesv

method leads to a cubic run-time complexity on the matrix size. Therefore, obtaining the steady-state probability has complexity  $\mathcal{O}(L_1^{3R})$ . Note that it is the computation of  $\mathbf{p}$  that dominates the complexity of approximating  $\lambda_n$ , as creating the transition matrix  $\mathbf{Q}$  has  $\mathcal{O}(RL_1^R)$  complexity and computing  $\pi_n$  has  $\mathcal{O}(L_1^R)$  complexity – see (5). Hence, the first approximation of  $\lambda_n$  has run-time complexity  $\mathcal{O}(L_1^{3R})$ .

### 6.2. Second approximation of $\lambda_n$

In (9) we see that there is a power relationship between  $n$  and  $\lambda_n$ , namely,  $\lambda_n = \mu(\frac{\Lambda}{n\mu})^n$ . As computing a power has complexity  $\mathcal{O}(\log n)$ , the second approximation of  $\lambda_n$  has complexity  $\mathcal{O}(\log n)$ .

### 6.3. First approximation of $A_n$

Once we compute the Markov chain steady-state probabilities  $p_n$ , this method only performs a summation over such probabilities (17). Thus, the complexity of computing  $A_n$  is  $\mathcal{O}(L_1^R)$ , for we iterate over all the  $L_1^R$  states and check whether each of them satisfies  $\min s_j = n$ .

### 6.4. Second approximation of $A_n$

Given the values of  $\lambda_n$ , first we compute the probability of joining the queue when there are 0 users  $A_0$  in (19). As mentioned in Section 5.7, we truncate the infinite summations up to  $L_2$ . Hence, it takes  $\sum_i^{L_2} i$  operations to compute  $A_0$ , and so is  $\mathcal{O}(L_2^2)$ . Once  $A_0$  is computed, we perform  $\mathcal{O}(L_2)$  operations to compute  $A_n$  in (18). Therefore as a whole, the second approximation of  $A_n$  has  $\mathcal{O}(L_2^2)$  complexity.

### 6.5. First approximation of $w_n(t)$

This approximation computes the exponential of the defective infinitesimal generator matrix  $D$  – see (20). As mentioned in Section 5.7, we also truncate the  $D$  matrix up to  $L_2$  elements in its diagonal such that  $D$  is an  $L_2 \times L_2$  matrix. As  $D$  is diagonal with  $\leq 3$  terms at each row, its creation has complexity  $\mathcal{O}(L_2)$ . With Padé's method (Arioli et al., 1996) we compute  $D$  exponential with  $\mathcal{O}(L_2 \log L_2)$  complexity.

### 6.6. Second approximation of $w_n(t)$

Using the recurrent formula of Lemma 1 we can check the complexity of this second approximation of  $w_n(t)$ . As mentioned in Section 5.7, we truncate the infinite summation in (22) to  $L_2$  iterations. At each summation iteration  $i$ , we perform  $\mathcal{O}(\log i)$  operations (the power operators), hence, computing the second approximation of  $w_n(t)$  has complexity  $\mathcal{O}(L_2 \log L_2)$ . Note that we compute  $h_{n,i}$  incrementally thanks to the recursive approach, hence, such computation does not dominate the approximation complexity as  $h_{n,i+1}$  reuses already computed values of  $h_{*,i}$ . Similarly, we also keep inside a hash table the factorial computations  $i!$  at (22) denominator to ease the computational burden.

Depending on which Method we use – see Table 2 – we will get different run-time complexities. Namely, methods A,B,D, and E have an  $\mathcal{O}(L_1^{3R})$  complexity because they rely

**Table 3**  
Complexity of each method.

Method	$\lambda_n$	$A_n$	$w_n(t)$	Overall
<b>A</b>	$\mathcal{O}(L_1^{3R})$	$\mathcal{O}(L_1^R)$	$\mathcal{O}(L_2 \log L_2)$	$\mathcal{O}(L_1^{3R})$
<b>B</b>	$\mathcal{O}(L_1^{3R})$	$\mathcal{O}(L_2^2)$	$\mathcal{O}(L_2 \log L_2)$	$\mathcal{O}(L_1^{3R})$
<b>C</b>	$\mathcal{O}(\log n)$	$\mathcal{O}(L_2^2)$	$\mathcal{O}(L_2 \log L_2)$	$\mathcal{O}(L_2^2)$
<b>D</b>	$\mathcal{O}(L_1^{3R})$	$\mathcal{O}(L_1^R)$	$\mathcal{O}(L_2 \log L_2)$	$\mathcal{O}(L_1^{3R})$
<b>E</b>	$\mathcal{O}(L_1^{3R})$	$\mathcal{O}(L_2^2)$	$\mathcal{O}(L_2 \log L_2)$	$\mathcal{O}(L_1^{3R})$
<b>F</b>	$\mathcal{O}(\log n)$	$\mathcal{O}(L_2^2)$	$\mathcal{O}(L_2 \log L_2)$	$\mathcal{O}(L_2^2)$

on the truncated Markov chain to derive  $\lambda_n$ , which is the most demanding approximation. While methods C and F have an overall complexity of  $\mathcal{O}(L_2^2)$  because the 5.2 and 5.6 approximations dominate the computation of  $W(t)$ . Table 3 summarises the computational complexity of each method.

### 6.7. Simulation

Events, and more importantly the number of events in a run of the simulation are random. Therefore we cannot have a true complexity analysis, but we can say something about the order of expected number of operations. In this section we consider the average time complexity of the M/M/R-JSQ-PS system.

We will consider number of operations per unit of simulation time when in steady state. Assuming there are  $M$  customers in the system at steady-state, there are two types of **B**-events that can take place in a given time unit, arrivals, and customers ending service.

- *Arrivals*: there's an average of  $\Lambda$  arrivals per time unit. At each arrival we need to check  $R$  servers to see which is least busy. Then once a server is chosen, we need to go through each customer at that server and re-schedule their end service dates - (1). As join-shortest-queue systems should evenly share customers between servers, we expect there to be  $\frac{M}{R}$  customers at that server. So per time unit, the expected number of operations for arrival events is  $\mathcal{O}\left(\Lambda \left(R + \frac{M}{R}\right)\right)$ .
- *End services*: at steady state, due to work conservation and Burke's theorem (Burke, 1956), there's an average of  $\Lambda$  services ending per time unit. At each end service we need to go through each customer at that server and re-schedule their end service dates. So per time unit, the expected number of operations for end service events is  $\mathcal{O}\left(\Lambda \frac{M}{R}\right)$ .

It is difficult to find a closed expression for  $M$ , hence the need for simulation and approximations. However a naive estimate for the average number of customers  $M$  is the traffic intensity,  $M \approx \rho = \frac{\Lambda}{\mu R}$ . Let  $q_{\max}$  be the maximum simulation time. Altogether, in steady state the expected number



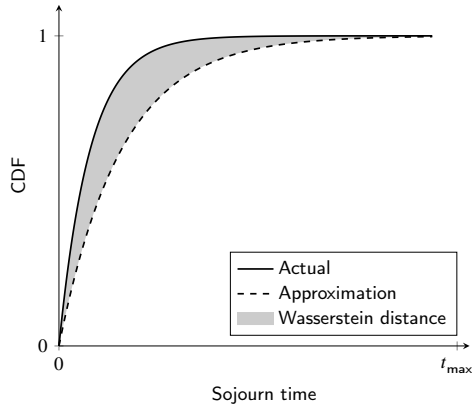


**Figure 5:** Graphical interpretation of the Wasserstein distance between the actual and approximated CDFs.

of operations is  $\mathcal{O}\left(q_{\max}\left(\Lambda\left(R + \frac{M}{R}\right) + \Lambda\frac{M}{R}\right)\right)$  for a simulation run, which is equivalent to  $\mathcal{O}\left(q_{\max}\left(\Lambda R^2 + \frac{2\Lambda^2}{\mu R^2}\right)\right)$ .

Although  $q_{\max}$  is a user chosen hyper-parameter, and increases the expected number of operations linearly, it is useful to consider if its choice should be influenced by other system parameters. Consider that, when in steady state, increasing the simulation time increases the number of sojourn time samples we have to estimate the CDF. Say we need  $X$  samples to estimate a good CDF, then  $q_{\max}$  should be chosen such that  $q_{\max} = \frac{X}{\Lambda}$ . As  $X$  is independent of any other parameter, it can be considered a constant. However, this is assuming a steady state. We should actually choose  $q_{\max} = \frac{X}{\Lambda} + q_{\text{warmup}}$ , where  $q_{\text{warmup}}$  is the warmup time, the time it takes to reach steady state. It is likely that  $q_{\text{warmup}}$  would be effected by the system parameters.

It is interesting to note that the six approximations' time complexities, and the expected time complexity for the simulation, are affected by different parameters. The approximations are affected by the hyper-parameters  $L_1$  and  $L_2$ , along with  $R$ , however the simulation is effected by the system parameters themselves. This shows that for some specific cases and parameter sets, it might be worthwhile resorting to simulation after all.

## 7. Approximations' accuracy

We perform a computational experiment to compare the six methods against one another under various circumstances. With a fixed choice of  $\mu = 1$  we calculate the sojourn time CDFs using each method, for all  $1 \leq R \leq 10$ , and all  $\rho \in (0, 1)$  in steps of 0.01. CDFs are compared against the simulation CDF using the Wasserstein distance (Mostafaei and Kordnourie, 2011), or Earth-mover's distance. This is given in (27), with a graphic interpretation given in Figure 5. This measure goes from 0, representing equal CDFs, to  $t_{\max}$ , the maximum sojourn time calculated, representing the largest possible difference between the CDFs. In practice this is calculated numerically by taking Riemann sums

**Table 4**

Choice of Markov chain limit  $L_1$  for each  $R$ .

$R$	$L_1$
1	22
2	22
3	22
4	13
5	7
6	5
7	4
8	3
9	3
10	2

with  $\Delta = 0.01$  time units.

$$\Omega(G, H) = \int_{-\infty}^{+\infty} |G(t) - H(t)| dt \quad (27)$$

For these experiments hyper-parameter choices are a fixed:  $L_2 = 130$ ;  $t_{\max} = 182.32$ ; a maximum simulation time of  $q_{\max} = 160000$  time units and a warm-up time of  $q_{\text{warmup}} = 8000$ . The choice of the Markov chain limit  $L_1$  is dependent on  $R$ , it is chosen to be both large enough that the probability of exceeding this is small, and small enough so that the number of defined transitions is manageable, we choose  $(L_1 + 1)^{2R} < 10 \times 10^{10}$ . For each  $R$  our choice of  $L_1$  is given in Table 4.

Figure. 6a-6f show the obtained Wasserstein distance, for each method A to F respectively, for each value of  $R$  and  $\rho$ .

First it is important to note the scale of the y-axis on these plots, they range from 0 to 2; while the Wasserstein distance has the potential to range from 0 to 182.32. Therefore, wherever the Wasserstein distance falls within the plot's range, we can note that these are not bad approximations overall. We can see that all methods are highly dependant on the traffic intensity  $\rho$ , however the relationship between accuracy and  $\rho$  is different for the methods that use the first approximation of  $w_n$  (methods A, B and C), and those that use the second approximation of  $w_n$  (methods D, E and F). For the first approximation, low and high values of the load  $\rho$  result in higher approximation error. This may be due to unstable approximation algorithms used to compute matrix exponential (Moler and Van Loan, 2003). While the second approximation performs much better for low values of  $\rho$ , middling values perform much worse here. In addition, we see that the second approximation is more dependant of  $R$ , with lower values of  $R$  performing better. Similarly, this dependence on  $R$  is more pronounced in methods C and F, suggesting that the second approximation of  $\lambda_n$  performs worse with higher  $R$  than the first Markov chain approximation.

Figure 7 shows which method was most accurate for each  $R, \rho$  pair. From this we see that method D performed best for low values of  $\rho$ , while method C performed best for middling to high values of  $\rho$ . Method E is the best performing methods

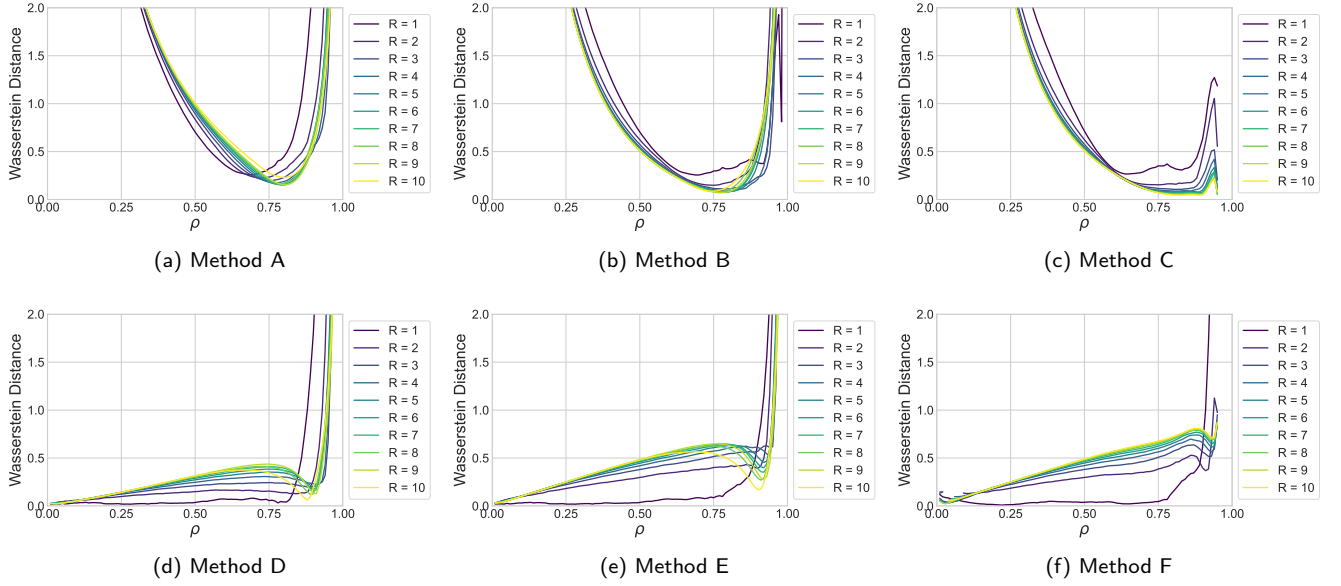


Figure 6: Accuracy of each method with increasing traffic intensity  $\rho$  and number of CPUs  $R$ .

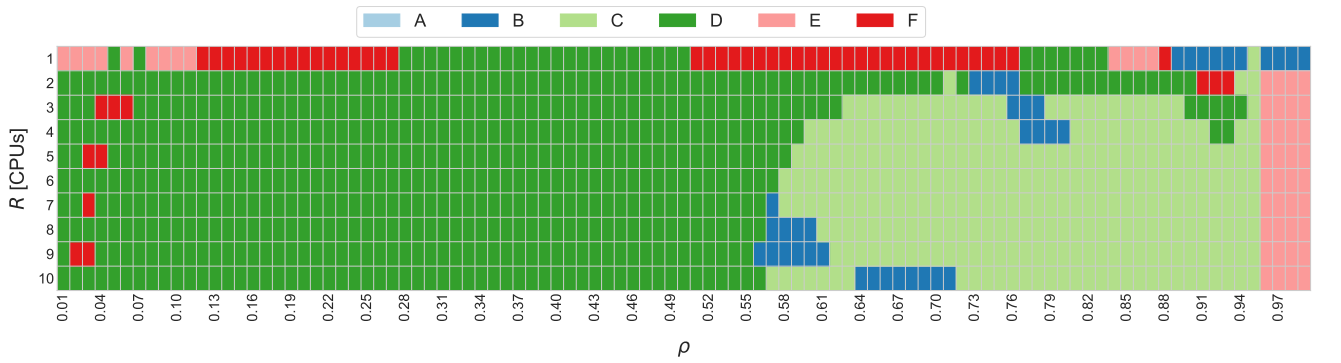


Figure 7: Most accurate method Table 2 for each  $R$ ,  $\rho$  pair.

for very high values of  $\rho$ , however from the plot in Figure 6e we know that these are still not good approximations of the CDF. Interestingly, when  $R = 1$ , that is when there is no join-shortest-queue behaviour happening, methods E, D and F are the best performing.

## 8. Behaviour in high reliabilities

In the prior section we have seen that methods A-F yield an accurate approximation of the sojourn time CDF, namely that the Wasserstein distance remains reasonably small. Depending on the load conditions  $\rho$  we can use the approximation with highest accuracy (see Figure 7) to achieve accurate sojourn time CDF approximations.

However, URLLC services ask for end-to-end latencies with high reliabilities as 99%, 99.9%, 99.99%, or 99.999%. This means that the network latency plus processing latency of a service (that is the sojourn time) should be met, e.g., 99.99% of the times. If the end-to-end latency requirement is of 100ms and the maximum network latency remains below

28ms, this means that the sojourn time should remain below 72ms in the 99.99% of the times. Therefore, the applicability of our methods A-F depend on their accuracy at the 99.99<sup>th</sup> percentile.

In Figure 8 we illustrate the error, measured in scalable time units, achieved by the best approximation at the 99.99<sup>th</sup> percentile. In other words, if  $T_{a,99.99}$  is the best method 99.99<sup>th</sup> percentile for the sojourn time, and  $T_{99.99}$  is the simulated 99.99-percentile; then Figure 8 illustrates  $T_{a,99.99} - T_{99.99}$ . To derive the simulated 99.99<sup>th</sup> percentile use to the simulation from Section 4,

As with the Wasserstein distance (see Figure. 6a-6f), Figure 8 evidences that the 99.99<sup>th</sup> error becomes more prominent as the load  $\rho$  approaches to 1 in the M/M/R-JSQ-PS system. In particular, the best method under-estimates the 99.99<sup>th</sup> percentile of the sojourn time for the error falls towards negative values near -175 as  $\rho$  approaches to 1. Note that the maximum sojourn time in the experiments can pop up to  $t_{\max} = 182.32$  time units, hence, the error is notoriously large towards the highest load  $\rho \approx 1$ .

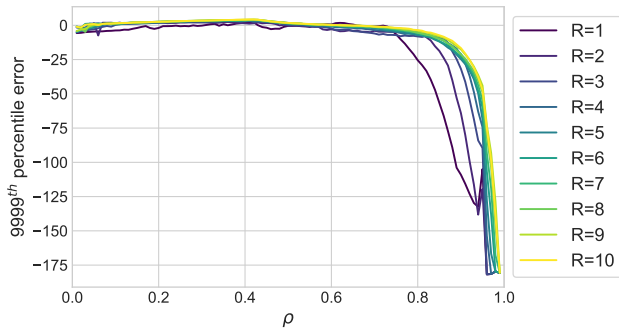


**Figure 8:** Sojourn time 99.99<sup>th</sup> percentile error using the best method. Positive/negative means over/under-estimation, respectively.

Nevertheless, for not so high loads the 99.99<sup>th</sup> percentile error remains low. Namely, the error is of less than  $t = 12$  time units with respect to the simulations when  $R \geq 3$  CPUs and  $\rho \leq 0.85$ , and less than  $t = 1.78$  time units when  $R \geq 3$  CPUs and  $\rho \leq 0.50$ . If the system has  $R < 3$  CPUs, then the best method has erratic oscillations, indeed the 99.99<sup>th</sup> percentile is underestimated by  $t = -56.6$  time units with  $R = 1$  and  $\rho = 0.85$  – see Table 5.

We have also analysed what is best method error for the 99<sup>th</sup>, 99.9<sup>th</sup>, and 99.999<sup>th</sup> percentiles. The results are shown in Appendix A and they show the same pattern as the observed for the 99.99<sup>th</sup> percentile in Figure 8. That is, the best A-F method results in under-estimations of the sojourn time that get worse as  $\rho$  approaches to 1. Moreover, the results from Figure 10 in Appendix A shows that the error oscillations start to become more prominent with higher reliabilities and mid values of CPUs.

Overall, the best method gives accurate estimations for the 99.99<sup>th</sup> percentile of the sojourn time as long as  $\rho \leq 0.85$ ; tends under-estimate the 99.99<sup>th</sup> percentile; and is more stable for  $R \geq 3$  CPUs.

### 8.1. Comparison with non-exponential service times

So far we have seen that the methods A-F perform sufficiently well to estimate high reliabilities of an M/M/R-JSQ-PS system, e.g., the 99.99<sup>th</sup> percentile of the sojourn time. However, exponentially distributed service rates are often an unrealistic assumption, with uniformly distributed or deterministic service times being more realistic for services with a bounded number of operations. Here we explore the use of our best M/M/R-JSQ-PS approximation to upper bound 99.99<sup>th</sup> percentiles of the sojourn time with uniform and deterministic service distributions. Such an upper bound is useful to tell whether  $R$  CPUs are enough to process URLLC service traffic, e.g., to tell if  $R$  CPUs process the URLLC service traffic in less than 28 ms with a 99.99% of probability.

To investigate, we calculate the compare sojourn time CDFs using exponentially distributed services and uniformly distributed and deterministic services, for various values of

**Table 5**

Sojourn time 99.99<sup>th</sup> percentile errors using the best method with increasing number of CPUs  $R$  and load  $\rho$ . Positive/negative mean over/under-estimation, respectively.

	$R = 1$	$R = 3$	$R = 5$	$R = 7$	$R = 10$
$\rho = 0.10$	-3.76	0.29	1.49	1.38	1.50
$\rho = 0.25$	-0.68	2.38	2.58	2.94	3.04
$\rho = 0.50$	-0.41	0.22	1.17	1.47	1.78
$\rho = 0.75$	-6.56	-7.15	-4.51	-3.04	-1.87
$\rho = 0.85$	-56.60	-8.83	-11.87	-9.84	-7.29
$\rho = 0.90$	-109.06	-31.78	-24.69	-20.86	-16.63
$\rho = 0.95$	-104.87	-89.57	-68.65	-54.94	-47.24
$\rho = 0.99$	-180.58	-180.59	-180.60	-180.61	-180.62

$R$  and  $\rho$ . All CDFs were obtained using the simulation using an exponential distribution with average service time  $\frac{1}{\mu}$ ; a uniform distribution  $U\left(\frac{1}{2\mu}, \frac{3}{2\mu}\right)$ ; and deterministic service time of  $\frac{1}{\mu}$  time units. In such a manner, all distributions share the same average service time, although their variances are not equal: the exponentially distributed times having the highest variance ( $1/\mu^2$ ), followed by the uniform distributed times ( $1/(12\mu^2)$ ), and then the deterministic with no variance.

We see that the CDFs obtained when modelling service times as exponentially distributed always lie below those obtained using uniformly distributed and deterministic service times. This is demonstrated in Figure 9, which shows that the tail percentiles are always larger, or more pessimistic, when modelling exponential services as opposed to uniform and deterministic services.

Figure 9 also evidences how near  $\rho = 0.6$  when we use  $R = 5$  or  $R = 10$  CPUs the best method (dark green) gets closer to the percentiles of the simulated results (yellow). This behaviour is because after  $\rho = 0.6$  the best method changes from method D to method C (see Figure 7). Similarly, at high loads  $\rho \geq 0.97$  the best method changes from C to E, thus, the sudden change in the sojourn time percentiles. Namely, the sojourn time percentiles at such high loads differs significantly from the values obtained in the simulation (yellow). The erratic values of the best method for  $\rho \geq 0.97$  even goes below the sojourn time percentiles obtained for uniform and deterministic service times (blue and red lines in Figure 9, respectively).

Altogether, Figure 9 shows: that our best method (dark green) stays close to the sojourn time percentiles obtained in simulations (yellow) for loads  $\rho < 0.97$ ; that our best method lies above the sojourn times provided by deterministic (red) and uniformly distributed (blue) service times; and that our best method largely underestimates the sojourn time percentile for  $\rho \geq 0.97$ , resulting in even smaller percentiles than uniformly distributed and deterministic service times.

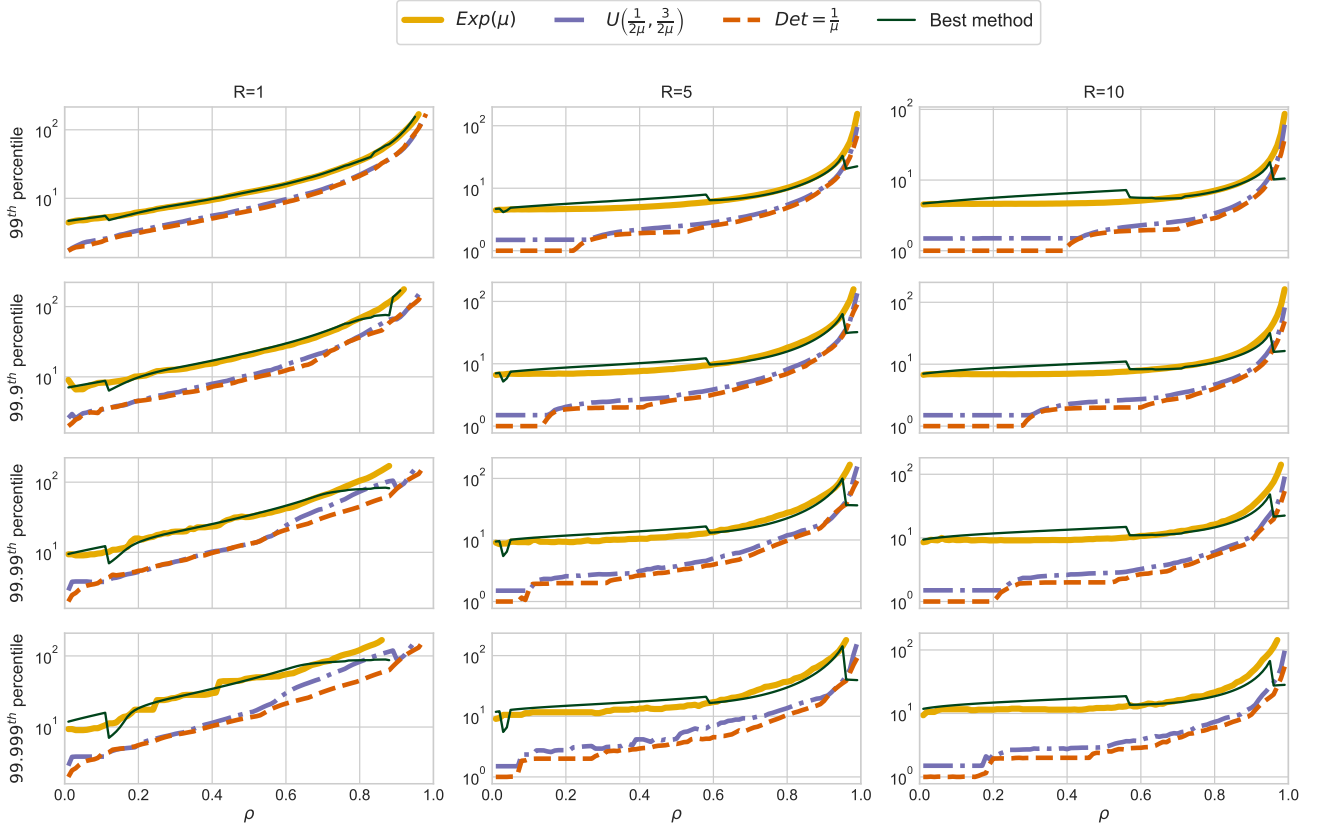


**Figure 9:** The 99th, 99.9th, 99.99th and 99.999th percentiles of the sojourn time distributions, on a log scale, when service times are modelled as exponentially distributed, uniformly distributed, and deterministic.

## 9. Conclusions

This paper models the M/M/R-JSQ-PS sojourn time distribution for URLLC services whose traffic is processed using a multi-processor PS system. In the paper we:

- i) present a generic open-source discrete event simulation software for G/G/R-JSQ-PS systems;
- ii) derive and compare six analytical approximations for the sojourn time CDF of M/M/R-JSQ-PS systems, and analyse their run time complexities; and
- iii) investigate the applicability of M/M/R-JSQ-PS models to M/G/R-JSQ-PS systems under both Uniform and Deterministic intended service times.

The proposed approximations have polynomial time complexities  $\mathcal{O}(L_1^{3R})$ , and are useful to determine if  $R$  CPUs are enough to meet the URLLC requirements under mid loads, for they yield errors of less than 1.78 time units in high percentiles as a 99.99%. For mid to high loads the error remains below 12 time units.

## Acknowledgements

This work has been partially funded by European Union's Horizon 2020 research and innovation programme under grant agreement No 101015956, and the Spanish Ministry of Economic Affairs and Digital Transformation and the European

Union-NextGenerationEU through the UNICO 5G I+D 6G-EDGEDT and 6G-DATADRIVEN.

## Appendix A. Errors for increasing reliabilities

Figure 10 shows the error for the best approximation A-F from the 99th up to the 99.999th percentile of the sojourn time. The sojourn time error is unitless, and it illustrates the increasing error as  $\rho$  approaches 1, so as the increasing oscillations of the error for higher reliabilities, even with mid values of the number of CPUs like  $R = 4$  – as explained in Section 8.

## Appendix B. Getting the sojourn time percentile

We provide an open-source implementation<sup>1</sup> of the proposed approximation methods A-F. Every method is implemented in Python and yields the sojourn time CDF for a given number of CPUs  $R$ . Additionally, it is possible to specify the truncation limits for the maximum number of customers considered at each CPU  $L_1$ , and the maximum number of customers at the system  $L_2$ .

In order to obtain the sojourn time  $\eta$ -percentile with  $R$  CPUs, we first compute the load  $\rho$  given the  $R$  CPUs, and

<sup>1</sup><https://github.com/geraintpalmer/mmr-jsq-ps/>



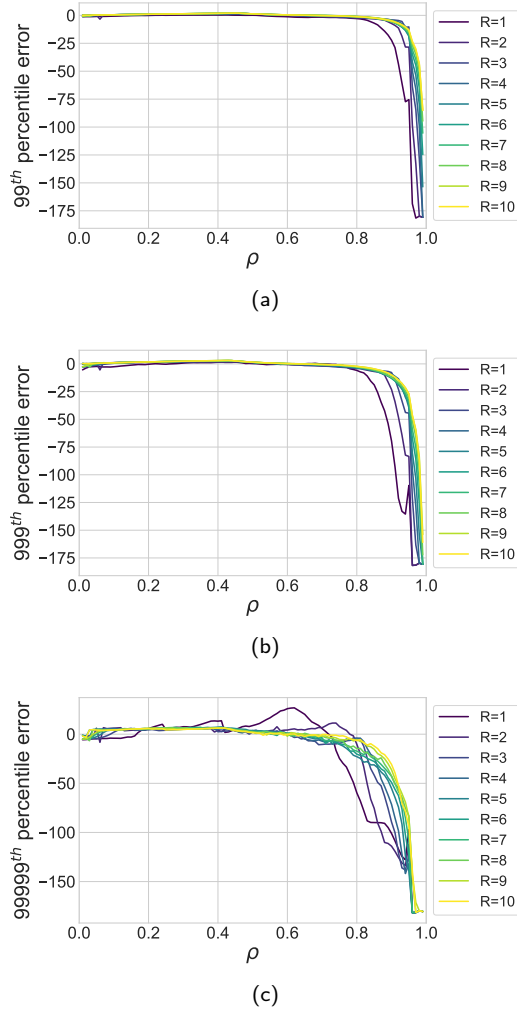


**Figure 10:** The best method error for the 99<sup>th</sup>, 99.9<sup>th</sup>, and 99.999<sup>th</sup> percentile the sojourn time. Positive/negative mean over/under-estimation, respectively.

the arrival and service rates  $\Lambda, \mu$ ; respectively. Second, we check Figure 7 to know which is the best method for the given  $(\rho, R)$  tuple, e.g., method-A. Third, we create an instance of method-A invoking

```
jsq.MethodA( $\Lambda, \mu, R, L_1, L_2, \{t_0, t_1, \dots\}$ )
```

with  $\{t_0, t_1, \dots\}$  being the discrete time points at which we compute the CDF. Then, we obtain the CDF of method-A by accessing property `sojourn_time_cdf` of the method instance. This property holds a vector  $\{P_0, P_1, \dots\}$  that represents the CDF computed by method-A. In particular, each element represents  $P_i = \mathbb{P}(T \leq t_i)$ . Finally, we obtain the  $\eta$ -percentile of the sojourn time (denoted as  $t^\eta$ ) as

$$t^\eta = \arg \min\{t_i : \mathbb{P}(T \leq t_i) > \eta\} \quad (28)$$

## References

- 3GPP, 2019a. Release 15 Description; Summary of Rel-15 Work Items. Technical Report (TR) 21.915. 3rd Generation Partnership Project (3GPP).
- 3GPP, 2019b. Study on enhancement of Ultra-Reliable Low-Latency Communication (URLLC) support in the 5G Core network (5GC). Technical Report (TR) 23.725. 3rd Generation Partnership Project (3GPP).
- 3GPP, 2021. Management and orchestration; Study on Network Slice Management Enhancement. Technical Report (TR) 28.811. 3rd Generation Partnership Project (3GPP).
- 3GPP, 2022a. 5G System; Application Function Event Exposure Service; Stage 3. Technical Specification (TS) 29.517. 3rd Generation Partnership Project (3GPP).
- 3GPP, 2022b. Procedures for the 5G System (5GS). Technical Specification (TS) 23.502. 3rd Generation Partnership Project (3GPP).
- 3GPP, 2022c. Study on scenarios and requirements for next generation access technologies. Technical Report (TR) 38.913. 3rd Generation Partnership Project (3GPP).
- 5G Americas, 2021. Vehicular connectivity: C-V2X & 5G. White Paper. 5G Americas.
- Acemoglu, A., Krieglstein, J., Caldwell, D.G., Mora, F., Guastini, L., Trimarchi, M., Vinciguerra, A., Carobbio, A.L.C., Hysenbelli, J., Delsanto, M., Barboni, O., Baggioni, S., Peretti, G., Mattos, L.S., 2020. 5G Robotic Telesurgery: Remote Transoral Laser Microsurgeries on a Cadaveri. *IEEE Transactions on Medical Robotics and Bionics* 2, 511–518. doi:10.1109/TMRB.2020.3033007.
- Albanese, A., Sciancalepore, V., Costa-Perez, X., 2021. SARDO: An Automated Search-and-Rescue Drone-based Solution for Victims Localization. *IEEE Transactions on Mobile Computing*, 1–1doi:10.1109/TMC.2021.3051273.
- Arioli, M., Codenotti, B., Fassino, C., 1996. The padé method for computing the matrix exponential. *Linear Algebra and its Applications* 240, 111–130. URL: <https://www.sciencedirect.com/science/article/pii/S024379594001901>, doi:[https://doi.org/10.1016/0024-3795\(94\)00190-1](https://doi.org/10.1016/0024-3795(94)00190-1).
- Aschenbrenner, D., Fritscher, M., Sittner, F., Krauß, M., Schilling, K., 2015. Teleoperation of an Industrial Robot in an Active Production Line. *IFAC-PapersOnLine* 48, 159–164. URL: <https://www.sciencedirect.com/science/article/pii/S2405896315009921>, doi:<https://doi.org/10.1016/j.ifacol.2015.08.125>. 2nd IFAC Conference on Embedded Systems, Computer Intelligence and Telematics CESCIT 2015.
- Burke, P.J., 1956. The output of a queuing system. *Operations research* 4, 699–704.
- Chitta, S., Sucan, I., Cousins, S., 2012. Moveit! [ros topics]. *IEEE Robotics & Automation Magazine* 19, 18–19. doi:10.1109/MRA.2011.2181749.
- Cohen, R., Lewin-Eytan, L., Naor, J.S., Raz, D., 2015. Near optimal placement of virtual network functions, in: *IEEE INFOCOM*.
- Demmel, J., 1989. LAPACK: a portable linear algebra library for supercomputers, in: *IEEE Control Systems Society Workshop on Computer-Aided Control System Design*, pp. 1–7. doi:10.1109/CACSD.1989.69824.
- Egorova, R., Zwart, B., Boxma, O., 2006. Sojourn time tails in the M/D/1 processor sharing queue. *Probability in the Engineering and Informational Sciences* 20, 429–446. doi:10.1017/S0269964806060268.
- Guimarães, C., Groshev, M., Cominardi, L., Zabala, A., Contreras, L.M., Talat, S.T., Zhang, C., Hazra, S., Mourad, A., de la Oliva, A., 2021. Deep: A vertical-oriented intelligent and automated platform for the edge and fog. *IEEE Communications Magazine* 59, 66–72. doi:10.1109/MCOM.001.2000986.
- Gupta, V., Harchol Balter, M., Sigman, K., Whitt, W., 2007. Analysis of join-the-shortest-queue routing for web server farms. *Performance Evaluation* 64, 1062–1081. URL: <https://www.sciencedirect.com/science/article/pii/S0166531607000624>, doi:<https://doi.org/10.1016/j.peva.2007.06.012>. performance 2007.
- Harchol-Balter, M., 2013. *Performance modeling and design of computer systems: queueing theory in action*. Cambridge University Press.
- IEEE, 2021a. IEEE P802.11be/D1.0 Draft Standard for Information technology – Telecommunications and information exchange between systems Local and metropolitan area networks – Specific requirements. Part 11: Wireless LAN Medium Access Control (MAC) and Physical Layer (PHY) Specifications. Amendment 8: Enhancements for extremely high throughput (EHT). *IEEE Std 802.11ax-2021 (Amendment to IEEE Std 802.11-2020)*.
- IEEE, 2021b. *IEEE Standard for Information Technology–*

- Telecommunications and Information Exchange between Systems Local and Metropolitan Area Networks—Specific Requirements Part 11: Wireless LAN Medium Access Control (MAC) and Physical Layer (PHY) Specifications Amendment 1: Enhancements for High-Efficiency WLAN. IEEE Std 802.11ax-2021 (Amendment to IEEE Std 802.11-2020), 1–767doi:10.1109/IEEESTD.2021.9442429.
- Jemaa, F.B., Pujolle, G., Pariente, M., 2016. QoS-aware VNF placement optimization in edge-central carrier cloud architecture, in: 2016 IEEE Global Communications Conference (GLOBECOM), IEEE. pp. 1–7.
- Kempf, J., IAB, Austein, R., 2004. The Rise of the Middle and the Future of End-to-End: Reflections on the Evolution of the Internet Architecture. RFC 3724. URL: <https://www.rfc-editor.org/info/rfc3724>, doi:10.17487/RFC3724.
- Kleinrock, L., 1977. Queueing Systems, Volume 2: Computer applications. Wiley Online Library.
- Li, X., 2011. Radio Access Network Dimensioning for 3G UMTS. Springer.
- Liu, Y.C., Khong, M.H., 2015. Adaptive control for nonlinear teleoperators with uncertain kinematics and dynamics. IEEE/ASME Transactions on Mechatronics 20, 2550–2562. doi:10.1109/TMECH.2015.2388555.
- Masuyama, H., Takine, T., 2003. Sojourn time distribution in a MAP/M/1 processor-sharing queue. Operations Research Letters 31, 406–412.
- Moler, C., Van Loan, C., 2003. Nineteen dubious ways to compute the exponential of a matrix, twenty-five years later. SIAM review 45, 3–49.
- Mostafaei, H., Kordnourie, S., 2011. Probability metrics and their applications. Applied Mathematical Sciences 5, 181–192.
- Oljira, D.B., Grinnemo, K.J., Taheri, J., Brunstrom, A., 2017. A model for QoS-aware VNF placement and provisioning, in: 2017 IEEE Conference on Network Function Virtualization and Software Defined Networks (NFV-SDN), IEEE. pp. 1–7.
- Ott, T.J., 1984. The Sojourn-Time Distribution in the M/G/1 Queue with Processor Sharing. Journal of Applied Probability 21, 360–378. URL: <http://www.jstor.org/stable/3213646>.
- Palm, C., 1943. Variation in intensity in telephone conversations. Applied Probability Trust , 1–89.
- Palmer, G., 2018. Modelling deadlock in queueing systems. Ph.D. thesis. Cardiff University.
- Palmer, G.I., Knight, V.A., Harper, P.R., Hawa, A.L., 2019. Ciw: An open-source discrete event simulation library. Journal of Simulation 13, 68–82.
- Robinson, S., 2014. Simulation: the practice of model development and use. Palgrave Macmillan.
- Schweitzer, P., 1996. Stochastic Models, an Algorithmic Approach, by Henk C. Tijms (Chichester: Wiley, 1994), 375 pages, paperback. Probability in the Engineering and Informational Sciences 10, 463–464.
- SIMUL8 Corporation., 2022. Simul8. <https://www.simul8.com/>.
- Team SimPy, 2022. Simpy. <https://simpy.readthedocs.io/>.
- The AnyLogic Company, 2022. Anylogic. <https://www.anylogic.com/>.
- Ucar, I., Smeets, B., Azcorra, A., 2019. simmer: Discrete-event simulation for r. Journal of Statistical Software 90, 1–30. URL: <https://www.jstatsoft.org/index.php/jss/article/view/v090i02>, doi:10.18637/jss.v090.i02.
- Zhang, J., Dai, J., Zwart, B., 2009. Law of large number limits of limited processor-sharing queues. Mathematics of Operations Research 34, 937–970.



Geraint I. Palmer graduated from Aberystwyth University in 2013 with a BSc in mathematics, and then moved to Cardiff University to obtain his MSc in operational research and applied statistics in 2014, and his PhD in applied stochastic modelling in 2018, for which he won the OR Society's Doctoral Award. He now works as a lecturer at Cardiff University where his research is in operational research, queueing models and discrete event simulation.



Jorge Martín Pérez obtained a B.Sc in mathematics, and a B.Sc in computer science, both at Universidad Autónoma de Madrid (UAM) in 2016. He obtained his M.Sc. and Ph.D in Telematics from Universidad Carlos III de Madrid (UC3M) in 2017 and 2021, respectively. His research focuses in optimal resource allocation in networks, and since 2016 he participates in EU funded research projects in UC3M Telematics department.